J. Cell. Mol. Med. Vol 13, No 5, 2009 pp. 887-895

The pro-apoptotic protein Par-4 facilitates vascular contractility by cytoskeletal targeting of ZIPK

Susanne Vetterkind [a, b], Kathleen G. Morgan [a, b, *]

[a] *Boston Biomedical Research Institute, Watertown, MA, USA*
[b] *Department of Health Sciences, Sargent College of Health and Rehabilitation Sciences, Boston University, Boston, MA, USA*

Received: March 14, 2008; Accepted: April 30, 2008

Abstract

Par-4 (prostate apoptosis response 4) is a pro-apoptotic protein and tumour suppressor that was originally identified as a gene product up-regulated during apoptosis in prostate cancer cells. Here, we show, for the first time, that Par-4 is expressed and co-localizes with the actin filament bundles in vascular smooth muscle. Furthermore, we demonstrate that targeting of ZIPK to the actin filaments, as observed upon PGF-2 α stimulation, is inhibited by the presence of a cell permeant Par-4 decoy peptide. The same decoy peptide also significantly inhibits PGF-2 α induced contractions of smooth muscle tissue. Moreover, knockdown of Par-4 using antisense morpholino nucleotides results in significantly reduced contractility, and myosin light chain and myosin phosphatase target subunit phosphorylation. These results indicate that Par-4 facilitates contraction by targeting ZIPK to the vicinity of its substrates, myosin light chain and MYPT, which are located on the actin filaments. These results identify Par-4 as a novel regulator of myosin light chain phosphorylation in differentiated, contractile vascular smooth muscle.

Keywords: Par-4 • ZIPK • smooth muscle contractility • myosin light chain phosphorylation • myosin phosphatase

Introduction

Smooth muscle contraction in the vasculature is a key determinant of blood pressure and blood flow. A major mechanism of initiation of smooth muscle contraction is phosphorylation of the regulatory myosin light chain (LC20), which is largely determined by the opposing activities of myosin light chain kinase (MLCK) and myosin phosphatase. The myosin phosphatase holoenzyme is a heterotrimer composed of the 38 kD protein phosphatase 1 (PP1) catalytic subunit, a 110–133 kD myosin phosphatase target subunit (MYPT1), also termed myosin binding subunit (MBS), and a 20 kD subunit of unknown function [1]. While initially assumed to be constitutively active, myosin phosphatase is now considered as regulated by various pathways, most of which lead to inhibition of myosin phosphatase by phosphorylation of MYPT1 at threonine-696 and/or threonine-850. The kinases that have been implicated in inhibitory phosphorylation of MYPT1 are ROCK [2, 3], ILK [4] and ZIPK [5, 6]. ZIPK is expressed in various smooth muscle tissues such as intestine, vascular tissues and bladder, where it is associated with the regulatory subunit of myosin phosphatase, MYPT1 [5, 6].

In the process of investigating signalling pathways involved in regulation of smooth muscle myosin phosphatase, the pro-apoptotic protein Par-4 (prostate apoptosis response-4) attracted our interest, since Par-4 has been shown to interact with ZIPK in non-contractile cells [7, 8]. Par-4 was originally identified as the product of a gene that is up-regulated upon ionomycin-induced apoptosis in prostate cancer cells [9]. Subsequent reports also characterized Par-4 chiefly as a proapoptotic protein. Loss of Par-4 function was found to play a role in tumourigenesis, identifying the protein as a tumour suppressor. On the other hand, up-regulation of Par-4 has been linked to neuronal apoptosis in neurodegenerative diseases like amyoloid lateral sklerosis (ALS) and Alzheimer's disease, and in animal models of Parkinson's disease and Huntington's disease [10].

In the setting of apoptosis in non-muscle cells, the Preuss group [11] has shown that Par-4 targets ZIPK to the cytoskeleton, leading to apoptosis. In the same study, an increased LC20 phosphorylation

*Correspondence to: Kathleen G. MORGAN,
635 Commonwealth Ave.,
Boston, MA 02215, USA.
Tel.: 617-353-7464; Fax: 617-353-7567;
E-mail: kmorgan@bu.edu

doi: 10.1111/j.1582-4934.2008.00374.x

was also observed, but a cause-and-effect relationship was not shown. Here, we have suggested (1) that Par-4 modulates the ZIPK-mediated regulation of myosin phosphatase in general; and, (2) that Par-4 specifically regulates the contractility of fully differentiated vascular smooth muscle. We show here, that Par-4 is expressed at high protein levels in contractile, differentiated vascular smooth muscle (dVSM). The data presented in this manuscript show that Par-4 facilitates smooth muscle contraction, and acts as a cytoskeletal scaffold for ZIPK, dynamically targeting the kinase to the vicinity of its substrates, LC20 and MYPT1. Our results identify Par-4 as a novel regulator of LC20 phosphorylation and hence, contractility, in smooth muscle.

Material and methods

Tissue and cell preparation

All procedures were performed according to protocols approved by the Institutional Animal Care and Use Committee. Male ferrets (*Mustela putorius furo*, Marshall Farms, North Rose, NY) were killed by an overdose of chloroform, and tissues were prepared as previously described [12, 13]. Ferret tissues were used in this study because of the increased similarity of ferret proteins and physiological functions to the human relative to rodents [14–16].

Cell culture and transfection

A7r5 rat aorta cells were cultured in DMEM high glucose (Invitrogen) with 10% FCS, 1% glutamine, 50 units/ml penicillin and 50 μg/ml streptomycin. Cells were transiently transfected with a GFP-tagged ZIPK construct [17] performed with the jetPEI transfection reagent (PolyPlus, Illkirch, France). Transfected cells were subjected to a 24 hrs serum starvation prior to preparation of cell extracts.

Digital imaging

Cells were fixed, stained and analyzed as described previously [13]. As primary antibodies, the rabbit polyclonal anti-ZIPK (1:1000, Biomol) and anti-Par-4 (1:1000, Sigma) antibodies were used. As secondary antibodies, goat anti-rabbit Alexa Fluor® 488 and Alexa Fluor® 568 (1:1000, Molecular Probes) were used. Filamentous actin was stained with Alexa Fluor® 568 phalloidin (1:500, Molecular Probes).

Co-immunoprecipitation and pull-down experiments

A7r5 cells were lysed in isotonic lysis buffer and subjected to immunoprecipitation with the mouse monoclonal anti-Par-4 antibody (Santa Cruz Biotechnology, Inc., Santa Cruz, CA, USA). The antigen–antibody complexes were adsorbed to Protein G-Agarose (Sigma-Aldrich Co., St. Louis, MO, USA). For testing of the Par-4 decoy peptide, recombinant purified Par-4 protein [11] immobilized on StrepTactin beads (IBA, Göttingen, Germany) was incubated with extracts from GFP-ZIPK transfected A7r5 cells in the absence or presence of 10 μmol/L Par-4 decoy peptide or scrambled control peptide. Samples were washed three times with lysis buffer and analyzed by western blotting.

Immunoblotting

Samples were separated on 10% polyacrylamide gels according to standard procedures or on urea gels as described previously [12], and transferred to polyvinylidene difluoride (PVDF) membranes. The membranes were stained with anti-ZIPK or anti-Par-4 in the same dilutions as described above, or with the following antibodies: mouse monoclonal, anti-Tubulin α (1:3000, Santa Cruz), anti-LC20 (1:1500, Sigma), anti-Vimentin (1:1000, Sigma); rabbit polyclonal, anti-MYPT1 (1:2000, Covance), anti-phospho-MYPT1 T850 (1:1000, Upstate), anti-actin (1:2000, Cytoskeleton). Goat Oregon Green® 488 or Alexa Fluor® 568 labelled anti-rabbit or antimouse IgG were used as secondary antibodies (1:1000, Calbiochem). Bands were visualized on a Bio-Rad PhosphorImager. Densitometry analysis was performed with the MultiAnalyst software. Ponceau staining was used to verify equal protein loading and transfer.

Peptide interference experiments

Experiments were carried out with peptides consisting of the HIV TAT sequence (GYGRKKRRQRRR) to facilitate cellular peptide uptake as previously described [18], followed by either a sequence derived from the Par-4 leucine zipper motif (LKQENKTLLKVVGQLTR, decoy peptide), or a corresponding scrambled sequence (TVLKGVLNTRQLQKKEL, control peptide). Peptides were N-terminally tagged with fluorescein isothiocyanate (FITC). For immunofluorescence experiments, cells were incubated on ice for 1 hr with 10 μmol/L peptide solution in Ca^{2+}/Mg^{2+} free HBSS. For force transduction experiments, portal vein strips were incubated at 37°C with 50 μmol/L peptide in oxygenated PSS for 3 hrs.

Antisense experiments

Morpholino oligonucleotides were purchased from Gene Tools, LLC (Philomath, OR). Par-4 protein expression was suppressed using the antisense morpholino oligonucleotide 5′-CGGTAGCCACCGGTCGCCATATTCC-3′ complementary to the 5′ part of the ferret Par-4 gene including the initiation codon (underlined). The scrambled morpholino nucleotide 5′-CGCCGTGTCTGATCTTCGTGCATCC-3′ served as control. Ferret portal vein strips were chemically loaded with the morpholino oligonucleotides at 50 μmol/L performed with a previously described protocol [12]. On the fifth day of organ culture after loading, the muscle strips were quick-frozen following contractility assessment.

Quantification of filament association

Cells were analyzed by confocal fluorescence microscopy using the anti-ZIPK antibody. In three individual experiments, cells were categorized

as showing a filamentous or non-filamentous ZIPK staining pattern. The staining pattern was considered filamentous when at least two filaments of at least 5 μm length were visible. All cells on each coverslip were analyzed without bias. The percentage of cells showing a filamentous staining pattern was calculated from the total number of analyzed cells.

Solutions and materials

PSS contained (in mmol/L) 120 NaCl, 5.9 KCl, 2.5 $CaCl_2$, 1.2 $MgCl_2$, 25 $NaHCO_3$, 1.2 NaH_2PO_4 and 11.5 dextrose at pH 7.4 when bubbled with 95% O_2 5% CO_2. HBSS contained (in mmol/L) 137 NaCl, 5.4 KCl, 0.44 KH_2PO_4, 0.42 NaH_2PO_4, 4.17 $NaHCO_3$, 5.55 glucose and 10 HEPES [4-(2-hydroxyethyl)-1-piperazineethanesulfonic acid], pH 7.4. PBS-Tween solution contained (in mmol/L) 80 Na_2HPO_4, 20 NaH_2PO_4, 100 NaCl and 0.05% Tween. Isotonic lysis buffer contained (in mmol/L) 10 $NaPO_4$, pH 8.0, 140 NaCl, 3 $MgCl_2$, 1 dithiothreitol and 0.5% Nonidet-P40.PGF-2α was purchased from Sigma. General laboratory reagents were of analytical grade or better and were purchased from Sigma and Fisher Scientific.

Statistics

All values given in the text are mean ± SE. Differences between means were evaluated using a two-tailed Student's *t*-test. Significant differences were taken at the $P < 0.05$ level. For MYPT1 and LC20 phosphorylation levels, a one-tailed *t*-test was used, since based on contraction data from the same experiments, only reduction of phosphorylation was predicted for the antisense treated samples.

Results

Par-4 and ZIPK are expressed in vascular smooth muscle

After testing for antibody specificity (Fig. 1A), western blot analysis (Fig. 1B) demonstrates a strong expression of Par-4 in aorta, portal vein and trachea tissue, and weaker expression in brain, kidney, liver and lung. In kidney, a small band of 30 kD, probably representing a smaller splice isoform of Par-4 that has been described recently [19], is also present. ZIPK protein expression is strongest in lung, liver, heart and portal vein, followed by brain, trachea and aorta The data clearly show that Par-4 is expressed at high levels in dVSM tissues, and open the possibility of a functional role for the Par-4/ZIPK interaction in dVSM. Since ZIPK has been implicated in regulation of myosin phosphatase [5, 6, 20, 21], portal vein was chosen for the following experiments, as in this tissue, inhibition of myosin phosphatase contributes significantly to contractility [13] and cells are readily enzymatically dispersed from this tissue.

Subcellular localization and interaction of Par-4 and ZIPK in vascular smooth muscle cells

We next analyzed the subcellular distribution of ZIPK and Par-4 in fully differentiated vascular smooth muscle cells (dVSMCs). For this purpose, we fixed freshly isolated cells in the absence of any stimulus and stained them with the anti-Par-4 antibody and the anti-ZIPK antibody, respectively. Actin filaments, as a marker of the contractile filaments, were co-stained with phalloidin. As shown in (Fig. 1C), Par-4 is localized along the actin filament bundles, while ZIPK (Fig. 1D) shows a diffuse staining of the cytoplasm.

To test for interaction of endogenous Par-4 and ZIPK in smooth muscle cells, we performed co-immunoprecipitation experiments. Since the antibody used for western blot and immuno-fluorescence staining of Par-4 is not suitable for immunoprecipitation experiments, we used the mouse monoclonal anti-Par-4 antibody. This antibody, however, failed to immunoprecipitate endogenous Par-4 from ferret tissue lysates. Since the antibody was raised against Par-4 of rat origin, we performed immunoprecipitation experiments using the rat aorta smooth muscle cell line A7r5. Figure 1E shows that endogenous ZIPK is coprecipitated upon immunoprecipitation of endogenous Par-4 with the anti-Par-4 antibody, demonstrating the in vivo interaction of the two proteins in smooth muscle cells.

ZIPK transiently associates with actin filaments after contractile stimulation

Since in resting dVSM cells, ZIPK and Par-4 stainings show only partial overlap, the question arises as to whether the colocalization increases upon stimulation. We therefore performed a detailed time course analysis of the Par-4 and ZIPK subcellular distributions in cells fixed after stimulation with PGF-2α. Par-4 is associated with actin filaments at all time-points analyzed (1 to 15 min, data not shown). ZIPK, however, consistently redistributes to the actin filaments 1 min after stimulation with PGF-2α, while at later time-points the staining pattern gradually changes to a morepronounced cell surface staining and reduced nuclear staining (Fig. 2A). Quantitation reveals that at 1-min PGF-2α stimulation, the percentage of cells with filamentous staining pattern is significantly increased compared to resting cells (70.08 ± 3.39% compared to 34.03 ± 4.03%, Fig. 2A, graph).

A Par-4 decoy peptide interferes with ZIPK redistribution

Next, we investigated whether Par-4 is involved in ZIPK redistribution in dVSMCs in a cause-and-effect manner. For this purpose,

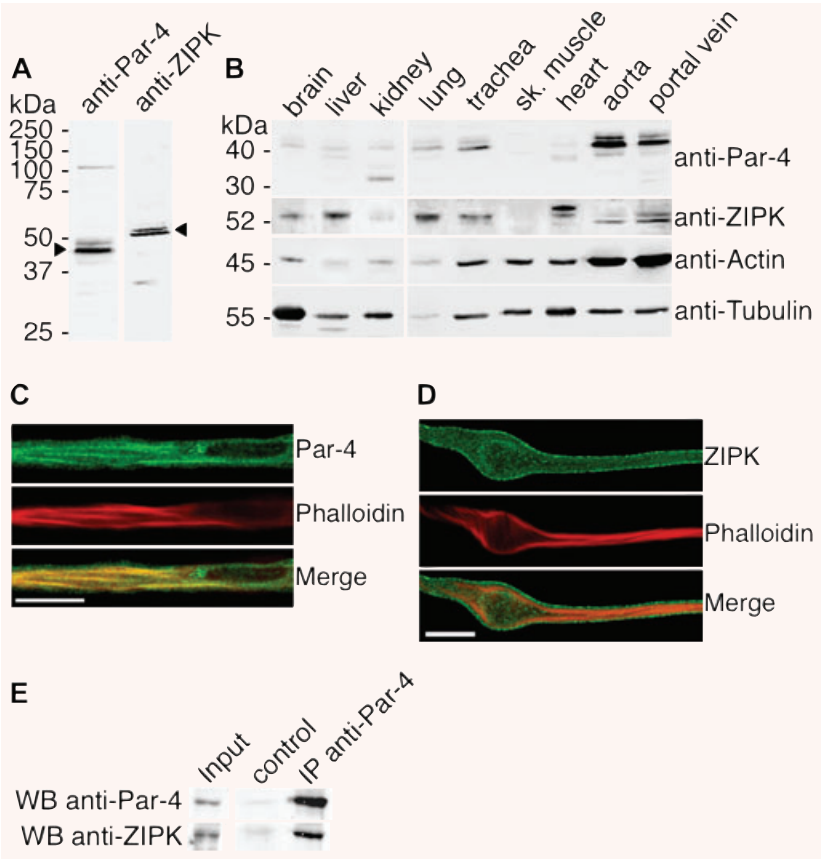

Fig. 1 ZIPK and Par-4 protein expression, subcellular localization and *in vivo* interaction. (**A**) Full-length western blots demonstrate specificity of the Par-4 and ZIPK antibodies. Portal vein lysates are shown here. (**B**) Homogenates from ferret tissues (10 μg total protein per lane) subjected to western blot analysis with anti-Par-4 and anti-ZIPK antibodies. The same membrane was stained with anti-actin and anti-tubulin antibodies to assess equal protein loading and transfer. (**C** and **D**) Confocal immunofluorescence imaging of dVSMCs performed with (**C**) anti-Par-4 and (**D**) anti-ZIPK antibodies. Filamentous actin was stained with phalloidin. Scale bar, 10 μm. (**E**) Endogenous Par-4 was immunoprecipitated from A7r5 cell lysates performed with the monoclonal anti-Par-4 antibody. Co-immunoprecipitated endogenous ZIPK was detected by western blotting. For the control sample, A7r5 lysates were incubated with beads only.

we designed and synthesized a cell permeant version of a Par-4 decoy peptide that contains amino acids 326–342 of Par-4 (see schematic drawing in Fig. 2B). The selected sequence is part of the C-terminal leucine zipper motif that has been shown to mediate the interaction between Par-4 and ZIPK as well as other Par-4 interaction partners [7, 22, 23]. By choosing this sequence, the decoy peptide was designed to compete with endogenous Par-4 in binding to ZIPK. Pull-down experiments were performed to test the efficacy of the decoy peptide. As shown in Figure 2C, the amount of ZIPK that bound to immobilized purified recombinant Par-4 protein was decreased in the presence of the Par-4 decoy peptide compared to that in the presence of the scrambled control peptide, or in the absence of peptides, demonstrating that the Par-4 decoy peptide interferes with the Par-4/ZIPK interaction and confirming that the decoy peptide can be used as a tool to disrupt the Par-4/ZIPK interaction.

Pre-treatment of cells with the decoy peptide before stimulation with PGF2α for 1 min inhibits the targeting of ZIPK to the actin filaments (Fig. 2D). Quantitative analysis shows that the percentage of cells with filamentous ZIPK staining pattern significantly decreases in the decoy peptide treated cells compared to the scrambled peptide treated cells.

The Par-4 decoy peptide and Par-4 knock down interfere with smooth muscle contractility

Our results predict that Par-4 targets ZIPK to the contractile filament bundles and to its substrates MYPT1 and LC20, thus presumably supporting contraction. To prove whether Par-4 indeed modulates contractility, we employed the previously described cell permeant Par-4 decoy peptide (see Fig. 2B) in force transduction experiments. Tissues were pre-treated with either the scrambled control peptide or with the decoy peptide prior to contractility assessment. Loading efficiency was monitored by immunofluorescence analyses of tissue pieces (data not shown). Compared to the control strips, contraction of the tissues treated with the decoy peptide is significantly reduced after 10-min PGF-2α stimulation (Fig. 3A). Although the effect is not large, consistent with the known redundancy of multiple signalling pathways in dVSM [24], it is highly statistically significant. Furthermore, the effect of the decoy peptide was specific for PGF-2α and also for KCl-induced contraction, since it had no effect on phenylephrine-induced contractility (data not shown).

As a second approach to analyze the contribution of Par-4 in smooth muscle contractility, we used antisense knockdown

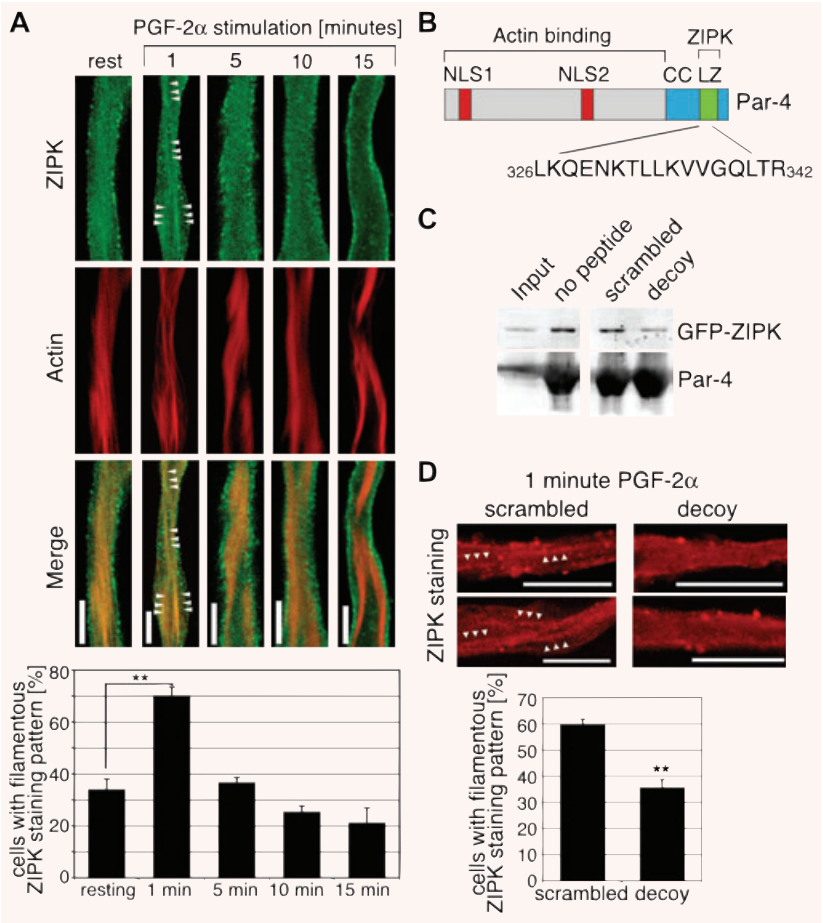

Fig. 2 A Par-4 decoy peptide inhibits the transient association of ZIPK with actin filaments. (**A**) dVSMCs were stimulated with 10 μmol/L PGF-2α or left untreated. Cells were fixed and stained for ZIPK and actin. Scale bars, 5 μm. Graph: The percentage of cells with filamentous staining pattern (showing two or more filaments of at least 5 μm length) is plotted against different time-points of PGF-2α stimulation. Values are averages from three independent experiments with a total of 44–54 cells per time-point. (**B**) Amino acid sequence of the decoy peptide and its position within the Par-4 protein. NLS1 and NLS2, nuclear localization signals; CC, coiled coil region; LZ, leucine zipper motif. (**C**) Control experiment showing peptide specificity. Immobilized Par-4 protein was incubated with extracts from GFP-ZIPK transfected A7r5 cells in the absence or presence of the Par-4 decoy peptide or the scrambled control peptide. ZIPK binding to the recombinant Par-4 protein, as detected by western blotting, is reduced in the presence of the Par-4 decoy peptide. (**D**) dVSMCs were incubated with scrambled or decoy peptides prior to stimulation with 10 μmol/L PGF-2α for 1 min. Cells were fixed and stained for ZIPK. Two representative cells are shown. Arrowheads highlight filamentous structures. Graph: the percentage of cells with filamentous ZIPK staining pattern was assessed in microscopy experiments. The graph shows the statistical analysis of three independent experiments with a total of 51–74 cells per peptide. Scale bars, 10 μm (**$P < 0.01$).

ofPar-4 with antisense morpholino nucleotides. On day five after morpholino loading in serum-free organ culture, the contractility of the treated tissues was significantly reduced (Fig. 3B). Thus, very similar results were obtained with two very different techniques.

The same tissue strips as used in the contractility assay following morpholino treatment were quick-frozen at the steady-state contraction and analyzed for protein expression. Western blot analysis after five days of organ culture shows that Par-4 protein levels were significantly reduced to 78.50 ± 3.91% (Fig. 3C, light grey bar) in the Par-4 antisense morpholino treated strips, while the level of MYPT1, vimentin and actin, which served as control proteins that were analyzed in parallel, remained at around 100% (Fig. 3C, black bars). To test our hypothesis that Par-4 promotes ZIPK translocation, thereby facilitating ZIPK-mediated phosphorylation of MYPT1 and LC20, we analyzed the phosphorylation of these ZIPK substrates in the morpholino-treated tissues For MYPT1, the threonine-850 phosphorylation site was chosen since its phosphorylation has been connected with detachment of MYPT1 from myosin [25], which may cause the agonist-induced redistribution of MYPT1 that has been previously observed in this same cell type [13]. Interestingly, a significant reduction of both MYPT1 and LC20 phosphorylation could be demonstrated: At steady-state contraction, MYPT1 phosphorylation at threonine-850 was reduced to 87.07 ± 5.22% in the antisense-treated strips compared to the control strips, and LC20 phosphorylation was reduced to 87.67 ± 4.67% (Fig. 3C, dark grey bars).

Discussion

Here, we demonstrate for the first time that Par-4 plays a role in the signalling pathways that regulate dVSM contractility. In summary, we provide evidence that (1) Par-4 is expressed at high protein levels in dVSM, (2) that it regulates targeting of zipper-interacting protein kinase, ZIPK, to its substrates MYPT1 and LC20 and (3) that phosphorylation levels of LC20 and MYPT1 as well as tissue contractility are decreased upon downregulation of Par-4 or decoy peptide interference, indicating a role for Par-4 in the regulation of contractility.

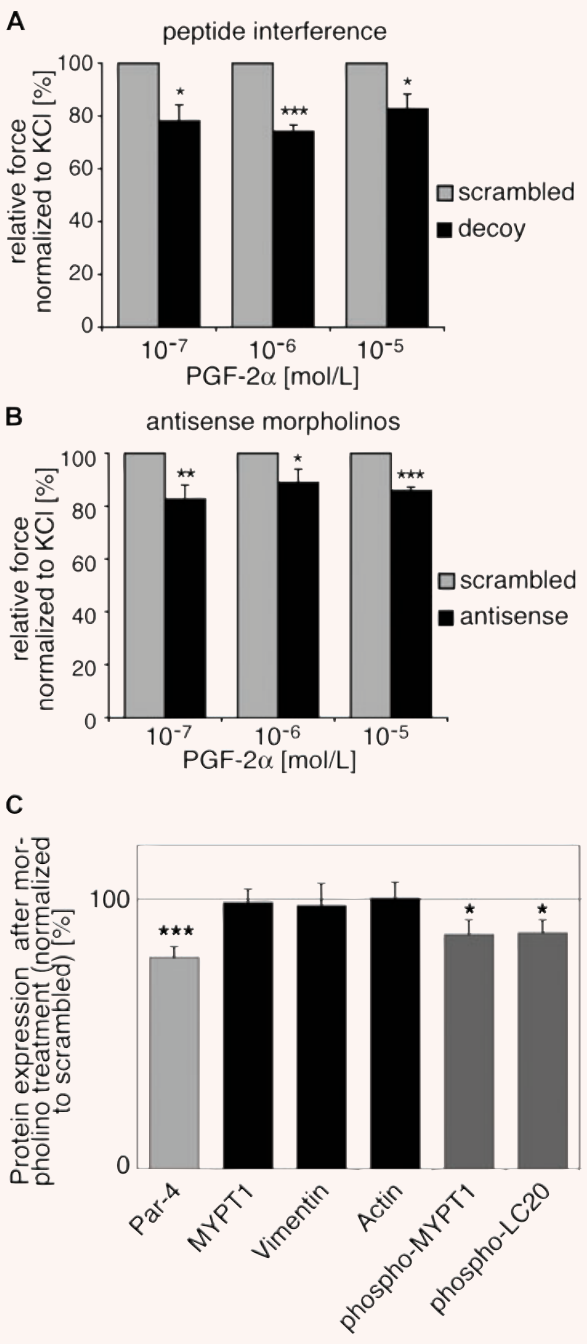

Fig. 3 Effect of Par-4 decoy peptide and Par-4 antisense morpholino treatment on tissue contractility. (**A**) Tissues were either treated with the Par-4 decoy peptide or a scrambled control peptide. Contractions were normalized to initial KCl contractions as assessed prior to peptide treatment. Six pairs of tissue strips, each pair from one ferret, were analyzed in individual experiments. Average contractions of the decoy peptide treated tissues in response to PGF-2α are shown as percentage of the scrambled peptide treated tissues (defined as 100%). (**B**) Tissue strips were either treated with Par-4 antisense morpholinos or scrambled control morpholinos. Contractions were normalized to KCl contractions on day two of organ culture experiments ($n = 8$; except 10^{-5} mol/L: $n = 6$). Average contractions of the antisense morpholino treated tissues in response to PGF-2α are shown as percentage of the scrambled morpholino treated control tissues (defined as 100%). (**C**) Antisense and scrambled morpholino treated tissues were frozen at the steady-state contraction following stimulation with PGF-2α. Protein levels were quantified by western blot analysis and densitometry performed with tubulin as reference protein. Par-4, MYPT1, Vimentin and Actin protein levels in the Par-4 antisense morpholino treated samples are shown as percentages of the control samples (light grey and black bars). For MYPT1 and LC20 phosphorylation levels (dark grey bars), the signals of the phospho-specific antibody (pMYPT) and the phosphorylated LC20 band (pLC20) were expressed as percentage of the corresponding total protein staining ($^{*}P < 0.05$; $^{**}P < 0.01$; $^{***}P < 0.001$).

A recent publication has suggested that the Par-4/ZIPK interaction is restricted to rodent cells [26]. However, our finding that Par-4 regulates the targeting and function of ZIPK and co-localizes with ZIPK argues against this concept. Clearly, the data presented here with contractile ferret smooth muscle cells show that ZIPK targeting by Par-4 is not restricted to rodent cells and are consistent with those of Kawai *et al.* [8], who have shown interaction of endogenous human Par-4 and ZIPK in HeLa cells.

The cause-and-effect relationship between Par-4 and regulation of contractility was shown by two different experimental approaches: (1) interference with Par-4 interactions by using a Par-4 decoy peptide, and (2) downregulation of Par-4 protein expression. We chose

to use antisense morpholino oligomers in this study, even though this method has not previously been reported for dVSM, because morpholinos are reported to be more stable, more specific and more effective than phosphorothioate nucleotides [27], which we have used in our previously published studies [12, 18, 28, 29]. It is worth noting that even with this approach, endogenous Par-4 protein was reduced by only 23%. Since sequences corresponding to the same Par-4 mRNA region have been successfully used in antisense experiments by various labs [30–32], we can exclude the possibility of ineffective targeting. The corresponding region of the ferret Par-4 mRNA was cloned and sequenced (data not shown) and proved to be 100% identical with the human Par-4 mRNA. The loading efficiency of the morpholinos was confirmed by visual and confocal inspection of the FITC signal (data not shown). The most likely factor affecting the degree of knock down is therefore the stability of the Par-4 protein. Protein stability is a general problem with antisense approaches in dVSM, since the rate of protein turnover is extremely low [33], so that even when mRNA translation is completely blocked, the efficiency of the knockdown approach still depends on the degradation of preexisting target protein. However, despite the challenge of using the antisense method in dVSM tissue, we were able to achieve significant downregulation of the Par-4 protein, and furthermore could show significant effects of the Par-4 downregulation on LC20 and MYPT1 phosphorylation levels and on tissue contractility.

It is noteworthy that another protein with a similar cytoskeletal scaffold function has been identified recently: the protein $p116^{RIP}$/M-RIP binds both RhoA and MYPT1, thus directing myosin phosphatase to the cytoskeleton [34–36]. The protein has been shown to participate in regulation of myosin phosphatase in various cell lines including aorta and coronary smooth muscle cells [36–38]. Both Par-4 and M-RIP may represent scaffold proteins that target myosin phosphatase to the contractile filament bundles and, upon stimulation, assemble it with one of its upstream kinases. Since the substrates of ROCK and ZIPK are overlapping and both kinases have similar consensus phosphorylation targets, specific binding of the Rho/ROCK complex to M-RIP and specific binding of ZIPK to Par-4 may mediate substrate specificity *in vivo* or lead to distinct subcellular localizations of Rho/ROCK and ZIPK, which might also result in different downstream effects. Alternatively, Par-4 and M-RIP might channel separate upstream pathways to the same downstream effect, thus potentiating MYPT1 phosphorylation and myosin phosphatase inhibition by the super-assembly of the Rho/ROCK pathway and the ZIPK pathway.

To the best of our knowledge, besides the data presented here, only one other non-apoptotic function for Par-4 has been described so far: the regulation of dopamine signalling in neuronal cells by interaction with the dopamine D2 receptor [39]. Apart from dopamine signalling, Par-4 has been associated with neuronal apoptosis and appears to be involved in the pathology of several neurodegenerative diseases [40]. We have analyzed the protein expression in different ferret tissues including brain, and found that, despite of the important role Par-4 seems to play in the nervous system, the protein expression in brain was low compared to vascular smooth muscle from aorta and portal vein. A possible explanation is that apoptotic stimuli trigger Par-4 protein expression in neuronal cells [31, 41, 42], while basal expression levels are kept low to protect the cells from accidental activation of the apoptotic response. However, it is intriguing that the high Par-4 protein expression in aorta and portal vein does not lead to induction of apoptosis. Our data show that the anti-apoptotic 30 kD splice isoform of Par-4 [19] is barely detectable in vascular smooth muscle and is therefore unlikely to account for this phenomenon. Thus, it is currently unclear what cellular signals ultimately determine whether Par-4 induces apoptosis or not. However, this will be important to resolve in future studies, should Par-4 have potential as a therapeutic target.

In summary, we have shown here that Par-4, although previously characterized mainly as a pro-apoptotic protein, supports contractility in dVSM. This novel role for Par-4 is associated with its capacity to target ZIPK to the cytoskeleton.

Acknowledgements

We thank Paul Leavis and his Peptide Core Facility for synthesizing the peptides. This study was supported by NIH grants HL31704 and HL80003 to K.G.M., and an Endre A. Balazs scholarship and an American Heart Association fellowship to S.V.

References

1. **Hartshorne DJ.** Myosin phosphatase: subunits and interactions. *Acta Physiol Scand.* 1998; 164: 483–93.
2. **Feng J, Ito M, Ichikawa K, Isaka N, Nishikawa M, Hartshorne DJ, Nakano T.** Inhibitory phosphorylation site for Rho-associated kinase on smooth muscle myosin phosphatase. *J Biol Chem.* 1999; 274: 37385–90.
3. **Kawano Y, Fukata Y, Oshiro N, Amano M, Nakamura T, Ito M, Matsumura F, Inagaki M, Kaibuchi K.** Phosphorylation of myosin-binding subunit (MBS) of myosin phosphatase by Rho-kinase *in vivo*. *J Cell Biol.* 1999; 147: 1023–38.
4. **Wilson DP, Sutherland C, Borman MA, Deng JT, Macdonald JA, Walsh MP.** Integrin-linked kinase is responsible for Ca2+-independent myosin diphosphorylation and contraction of vascular smooth muscle. *Biochem J.* 2005; 392: 641–8.
5. **MacDonald JA, Borman MA, Muranyi A, Somlyo AV, Hartshorne DJ, Haystead TA.** Identification of the endogenous smooth muscle myosin phosphatase-associated kinase. *Proc Natl Acad Sci USA.* 2001; 98: 2419–24.

6. **Endo A, Surks HK, Mochizuki S, Mochizuki N, Mendelsohn ME.** Identification and characterization of zipper-interacting protein kinase as the unique vascular smooth muscle myosin phosphatase-associated kinase. *J Biol Chem.* 2004; 279: 42055–61.
7. **Page G, Kogel D, Rangnekar V, Scheidtmann KH.** Interaction partners of Dlk/ZIP kinase: co-expression of Dlk/ZIP kinase and Par-4 results in cytoplasmic retention and apoptosis. *Oncogene.* 1999; 18: 7265–73.
8. **Kawai T, Akira S, Reed JC.** ZIP kinase triggers apoptosis from nuclear PML oncogenic domains. *Mol Cell Biol.* 2003; 23: 6174–86.
9. **Sells SF, Wood DP Jr, Joshi-Barve SS, Muthukumar S, Jacob RJ, Crist SA, Humphreys S, Rangnekar VM.** Commonality of the gene programs induced by effectors of apoptosis in androgen-dependent and -independent prostate cells. *Cell Growth Differ.* 1994; 5: 457–66.
10. **El-Guendy N, Rangnekar VM.** Apoptosis by Par-4 in cancer and neurodegenerative diseases. *Exp Cell Res.* 2003; 283: 51–66.
11. **Vetterkind S, Illenberger S, Kubicek J, Boosen M, Appel S, Naim HY, Scheidtmann KH, Preuss U.** Binding of Par-4 to the actin cytoskeleton is essential for Par-4/Dlk-mediated apoptosis. *Exp Cell Res.* 2005; 305: 392–408.
12. **Kim I, Je HD, Gallant C, Zhan Q, Riper DV, Badwey JA, Singer HA, Morgan KG.** Ca2+-calmodulin-dependent protein kinase II-dependent activation of contractility in ferret aorta. *J Physiol.* 2000; 526: 367–74.
13. **Shin HM, Je HD, Gallant C, Tao TC, Hartshorne DJ, Ito M, Morgan KG.** Differential association and localization of myosin phosphatase subunits during agonist-induced signal transduction in smooth muscle. *Circ Res.* 2002; 90: 546–53.
14. **Cavagna P, Menotti A, Stanyon R.** Genomic homology of the domestic ferret with cats and humans. *Mamm Genome.* 2000; 11: 866–70.
15. **Carson JL, Collier AM, Gambling TM, Hu SC.** An autoradiographic assessment of epithelial cell proliferation and post-natal maturation of the tracheal epithelium in infant ferrets. *Anat Rec.* 1999; 256: 242–51.
16. **Mackey MS, Stevens ML, Ebert DC, Tressler DL, Combs KS, Lowry CK, Smith PN, McOsker JE.** The ferret as a small animal model with BMU-based remodeling for skeletal research. *Bone.* 1995; 17: 191S–6S.
17. **Kögel D, Bierbaum H, Preuss U, Scheidtmann KH.** C-terminal truncation of Dlk/ZIP kinase leads to abrogation of nuclear transport and high apoptotic activity. *Oncogene.* 1999; 18: 7212–8.
18. **Marganski WA, Gangopadhyay SS, Je HD, Gallant C, Morgan KG.** Targeting of a novel Ca+2/calmodulin-dependent protein kinase II is essential for extracellular signal-regulated kinase-mediated signaling in differentiated smooth muscle cells. *Circ Res.* 2005; 97: 541–9.
19. **Wang G, Silva J, Krishnamurthy K, Bieberich E.** A novel isoform of prostate apoptosis response 4 (PAR-4) that co-distributes with F-actin and prevents apoptosis in neural stem cells. *Apoptosis.* 2006; 11: 315–25.
20. **Borman MA, MacDonald JA, Muranyi A, Hartshorne DJ, Haystead TA.** Smooth muscle myosin phosphatase-associated kinase induces Ca2+ sensitization via myosin phosphatase inhibition. *J Biol Chem.* 2002; 277: 23441–6.
21. **Haystead TA.** ZIP kinase, a key regulator of myosin protein phosphatase 1. *Cell Signal.* 2005; 17: 1313–22.
22. **Johnstone RW, See RH, Sells SF, Wang J, Muthukkumar S, Englert C, Haber DA, Licht JD, Sugrue SP, Roberts T, Rangnekar VM, Shi Y.** A novel repressor, par-4, modulates transcription and growth suppression functions of the Wilms' tumor suppressor WT1. *Mol Cell Biol.* 1996; 16: 6945–56.
23. **Diaz-Meco MT, Municio MM, Frutos S, Sanchez P, Lozano J, Sanz L, Moscat J.** The product of par-4, a gene induced during apoptosis, interacts selectively with the atypical isoforms of protein kinase C. *Cell.* 1996; 86: 777–86.
24. **Abdel-Latif AA.** Cross talk between cyclic nucleotides and polyphosphoinositide hydrolysis, protein kinases, and contraction in smooth muscle. *Exp Biol Med.* 2001; 226: 153–63.
25. **Velasco G, Armstrong C, Morrice N, Frame S, Cohen P.** Phosphorylation of the regulatory subunit of smooth muscle protein phosphatase 1M at Thr850 induces its dissociation from myosin. *FEBS Lett.* 2002; 527: 101–4.
26. **Shoval Y, Pietrokovski S, Kimchi A.** ZIPK: a unique case of murine-specific divergence of a conserved vertebrate gene. *PLoS Genet.* 2007; 3: 1884–93.
27. **Summerton J, Stein D, Huang SB, Matthews P, Weller D, Partridge M.** Morpholino and phosphorothioate antisense oligomers compared in cell-free and in-cell systems. Antisense Nucleic *Acid Drug Dev.* 1997; 7: 63–70.
28. **Gangopadhyay SS, Takizawa N, Gallant C, Barber AL, Je HD, Smith TC, Luna EJ, Morgan KG.** Smooth muscle archvillin: a novel regulator of signaling and contractility in vascular smooth muscle. *J Cell Sci.* 2004; 117: 5043–57.
29. **Je HD, Gangopadhyay SS, Ashworth TD, Morgan KG.** Calponin is required for agonist-induced signal transduction—evidence from an antisense approach in ferret smooth muscle. *J Physiol.* 2001; 537: 567–77.
30. **Sells SF, Han SS, Muthukkumar S, Maddiwar N, Johnstone R, Boghaert E, Gillis D, Liu G, Nair P, Monnig S, Collini P, Mattson MP, Sukhatme VP, Zimmer SG, Wood DP Jr, McRoberts JW, Shi Y, Rangnekar VM.** Expression and function of the leucine zipper protein Par-4 in apoptosis. *Mol Cell Biol.* 1997; 17: 3823–32.
31. **Guo Q, Fu W, Xie J, Luo H, Sells SF, Geddes JW, Bondada V, Rangnekar VM, Mattson MP.** Par-4 is a mediator of neuronal degeneration associated with the pathogenesis of Alzheimer disease. *Nat Med.* 1998; 4: 957–62.
32. **Bieberich E, MacKinnon S, Silva J, Noggle S, Condie BG.** Regulation of cell death in mitotic neural progenitor cells by asymmetric distribution of prostate apoptosis response 4 (PAR-4) and simultaneous elevation of endogenous ceramide. *J Cell Biol.* 2003; 162: 469–79.
33. **Lewis SE, Kelly FJ, Goldspink DF.** Pre- and post-natal growth and protein turnover in smooth muscle, heart and slow- and fast-twitch skeletal muscles of the rat. *Biochem J.* 1984; 217: 517–26.
34. **Mulder J, Poland M, Gebbink MF, Calafat J, Moolenaar WH, Kranenburg O.** p116Rip is a novel filamentous actin-binding protein. *J Biol Chem.* 2003; 278: 27216–23.
35. **Surks HK, Richards CT, Mendelsohn ME.** Myosin phosphatase-Rho interacting protein. A new member of the myosin phosphatase complex that directly binds RhoA. *J Biol Chem.* 2003; 278: 51484–93.
36. **Mulder J, Ariaens A, van den Boomen D, Moolenaar WH.** p116Rip targets myosin phosphatase to the actin cytoskeleton and is essential for RhoA/ROCK-regulated neuritogenesis. *Mol Biol Cell.* 2004; 15: 5516–27.
37. **Koga Y, Ikebe M.** p116Rip decreases myosin II phosphorylation by activating myosin light chain phosphatase and by inactivating RhoA. *J Biol Chem.* 2005; 280: 4983–91.

38. **Surks HK, Riddick N, Ohtani K.** M-RIP targets myosin phosphatase to stress fibers to regulate myosin light chain phosphorylation in vascular smooth muscle cells. *J Biol Chem.* 2005; 280: 42543–51.
39. **Park SK, Nguyen MD, Fischer A, Luke MP, Affar el B, Dieffenbach PB, Tseng HC, Shi Y, Tsai LH.** Par-4 links dopamine signaling and depression. *Cell.* 2005; 122: 275–87.
40. **Mattson MP, Duan W, Chan SL, Camandola S.** Par-4: an emerging pivotal player in neuronal apoptosis and neurodegenerative disorders. *J Mol Neurosci.* 1999; 13: 17–30.
41. **Chan SL, Tammariello SP, Estus S, Mattson MP.** Prostate apoptosis response-4 mediates trophic factor withdrawal-induced apoptosis of hippocampal neurons: actions prior to mitochondrial dysfunction and caspase activation. *J Neurochem.* 1999; 73: 502–12.
42. **Duan W, Rangnekar VM, Mattson MP.** Prostate apoptosis response-4 production in synaptic compartments following apoptotic and excitotoxic insults: evidence for a pivotal role in mitochondrial dysfunction and neuronal degeneration. *J Neurochem.* 1999; 72: 2312–22.